

Design of a compact wide-field-of-view infrared imager based on wavefront coding

Chonghui Zhu(朱崇辉), Jiaqian Yu(于佳倩), and Jingang Cui(崔金刚)
Citation: Chin. Phys. B, 2026, 35 (**2**): 024202. DOI: 10.1088/1674-1056/adf03f
http://cpb.iphy.ac.cn; http://iopscience.iop.org/cpb

What follows is a list of articles you may be interested in

Optical design of the time-resolved ARPES beamline of the new material spectroscopy experimental station for the update of CAEP THz-FEL facility

Liang-Liang Du(杜亮亮), Li-Min Meng(孟立民), Jiang Li(李江), and Li-Guo Zhu(朱礼国)
Chin. Phys. B, 2024, 33 (**11**): 114203. DOI: 10.1088/1674-1056/ad73b1

Design of three-dimensional imaging lidar optical system for large field of view scanning

Qing-Yan Li(李青岩), Yu Zhang(张雨), Shi-Yu Yan(闫诗雨),Bin Zhang(张斌), and Chun-Hui Wang(王春晖)
Chin. Phys. B, 2022, 31 (**7**): 074201. DOI: 10.1088/1674-1056/ac4a67

Simple and robust method for rapid cooling of ^{87}Rb to quantum degeneracy

Chun-Hua Wei(魏春华), Shu-Hua Yan(颜树华)
Chin. Phys. B, 2020, 29 (**6**): 064208. DOI: 10.1088/1674-1056/ab8625

Optical design of common-aperture multispectral and polarization optical imaging system with wide field of view

Xin Liu(刘鑫), Jun Chang(常军), Shuai Feng(冯帅), Yu Mu(穆郁), Xia Wang(王霞), Zhao-Peng Xu(徐兆鹏)
Chin. Phys. B, 2019, 28 (**8**): 084201. DOI: 10.1088/1674-1056/28/8/084201

Anti-detection technology of cat eye target based on decentered field lens

Da-Lin Song(宋大林), Jun Chang(常军), Yi-Fei Zhao(赵一菲), Ze-Xia Zhang(张泽霞)
Chin. Phys. B, 2018, 27 (**9**): 094220. DOI: 10.1088/1674-1056/27/9/094220

Design of a compact wide-field-of-view infrared imager based on wavefront coding

Chonghui Zhu(朱崇辉), Jiaqian Yu(于佳倩)†, and Jingang Cui(崔金刚)

Northeast Forestry University, Faculty of Science, Harbin 150040, *China*

(Received 8 May 2025; revised manuscript received 2 July 2025; accepted manuscript online 16 July 2025)

Compact size, high brightness, and wide field of view (FOV) are key requirements for long-wave infrared imagers used in military surveillance or night navigation. However, to meet the imaging requirements of high resolution and wide FOV, infrared optical systems often adopt complex optical lens groups, which will increase the size and weight of the optical system. In this paper, a strategy based on wavefront coding (WFC) is proposed to design a compact wide-FOV infrared imager. A cubic phase mask is inserted into the pupil plane of the infrared imager to correct the aberration. The simulated results show that, the WFC infrared imager has good imaging quality in a wide FOV of $\pm 16^{\circ}$. In addition, the WFC infrared imager achieves compactness with its 40 mm×40 mm×40 mm size. A fast focal ratio of 1 combined with an entrance pupil diameter of 25 mm ensures brightness. This work is of significance for designing a compact wide-FOV infrared imager.

Keywords: optical design, infrared imager, wavefront coding

PACS: 42.30.–d, 42.15.Fr, 95.85.Hp, 42.30.Va

DOI: 10.1088/1674-1056/adf03f **CSTR:** 32038.14.CPB.adf03f

1. Introduction

Infrared optical systems play an important role in scene perception and target recognition in applications such as military reconnaissance, industrial inspection and agricultural monitoring. To obtain a wider range of observation, extending the field of view (FOV) of infrared imaging optical systems has become a research object for many designers. To correct the aberrations introduced by the increase of FOV, the traditional design of optical systems is often complex. For example, Ye *et al*. designed a compact wide-FOV infrared imager based on off-axis two-mirror free-form surfaces.[1] This system exhibits excellent image quality within a wide FOV of 23°, but the off-axis reflection structure increases the difficulty of manufacturing and assembly. Li *et al*. proposed a folded large FOV scanning optical system, which overcomes the drawback of small mechanical scanning angle of MEMS lidar.[2] However, scanning systems tend to increase system size and reduce temporal resolution. In addition, Wu *et al*. proposed a design method for heterogeneous compound eye.[3] The camera prototype consists of 31 wide-angle sub-eyes and 226 high-definition sub-eyes, and has a large FOV ($360^{\circ} \times 141^{\circ}$) dual-scale imaging capability. But it greatly increases the difficulty of system design and puts great pressure on the system layout.

Small size, high brightness and wide FOV are key requirements for long-wave infrared imagers used in military surveillance or night navigation. In the long-wave infrared spectral range, the available materials with high transmittance are extremely limited. Limited by high-precision processing processes such as single crystal growth and diamond turning, the cost of these materials is significantly higher than that of visible and near-infrared optical materials.[4,5] Therefore, considering manufacturing costs, processing difficulties, and application value, a method needs to be proposed that can design an infrared imager with a wide FOV while minimizing the size of the system and the number of lenses.

Nowadays, in the performance improvements of optical imaging systems, computational imaging that combines optical design with computational algorithms has attracted widespread attention. The introduction of the computational imaging techniques alleviates the loading problem of optical devices effectively. As a typical representative of computational imaging techniques, wavefront coding (WFC)[6] follows the idea of transferring the burden of traditional optical system design to electronics and computer processing, and has been used in aberrations suppression of optical system widely.[7,8] Similar to polarization imaging in which micro-polarization array element is placed in the image plane of an optical system to modulate the polarization properties of the incident light,[9] WFC inserts a phase mask into the pupil plane to modulate the spatial phase distribution of the optical wavefront. By inserting a phase mask into the pupil plane of a traditional optical system, the image is encoded with a specific point spread function (PSF). Then, the encoded image is digitally restored with the de-convolution filter. The accurate image acquisition can be achieved even in the presence of optical aberrations. WFC reduces the complexity of optical systems, and provides new

†Corresponding author. E-mail: yujiaqian1992@126.com

© 2026 Chinese Physical Society and IOP Publishing Ltd. All rights, including for text and data mining, AI training, and similar technologies, are reserved.

ideas for aberration correction.

Recently, the application of WFC technology in infrared systems has become common. Feng *et al*. developed an athermalized WFC infrared imaging system and conducted quantitative experiments.[10] Results demonstrate that, compared to the traditional infrared imaging system, the WFC imaging system can output decoded images with sharpness over a wide temperature range of 110 °C. Zhou *et al*. extended the focus depth of a double bands infrared optical system by 10 times based on WFC technology and demonstrated WFC imaging experiments.[11] The test result shows that the decoded images at the 10 times defocus position maintain high resolution, verifying the feasibility of the WFC technology in suppressing defocus aberration. These validated WFC implementations provide the foundation for introducing this technology into the wide-FOV infrared imager design.

This paper introduces the application of WFC technology in designing a compact and wide-FOV infrared imager theoretically and experimentally. The paper is organized as follows: Section 2 illustrates the theoretical basis of WFC technology; Section 3 establishes a traditional infrared imager and analyzes its aberration characteristics; Section 4 shows the insensitivity of the WFC imaging system to aberrations and demonstrates the good imaging capabilities of the WFC infrared imager over a wide FOV; Section 5 summarizes the main findings of this work.

2. Theoretical basis of WFC technology

The basic principle of WFC technology is shown in Fig. 1. Compared with traditional imaging systems, WFC imaging system introduces a phase mask at the pupil plane of the system to encode the optical wavefront with a specific form of PSF so that obtains a blurred image with certain similarities, and then performs digital image processing on the encoded image. After image restoration, accurate image acquisition can be achieved even in the presence of optical aberrations.[6]

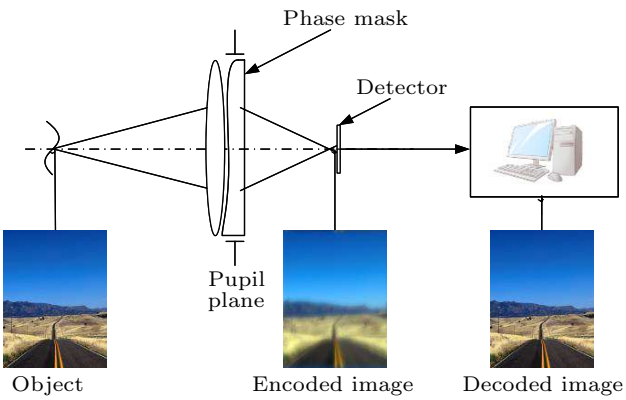


Fig. 1. Schematic diagram of WFC imaging system.

The PSF describes the output response of an optical system to a point light source. According to Fourier optics, without considering noise, the physical process of imaging can be described as the convolution of the object-space target and the PSF of the optical system. WFC sacrifices energy concentration to extend the support domain of PSF, thus reducing the sensitivity of the system to defocus.[12] The normalized spatial pupil function $P(x,y)$ of WFC system in the defocus state is

$$P(x,y) = \exp\{\mathrm{i}[\varphi_0(x,y)+\varphi(x,y)+\psi(x,y)]\}, \quad x^2+y^2 \le 1, \tag{1}$$

where (x,y) are spatial domain coordinates, φ_0 and φ are the phase distributions of the original optical system and the phase plate respectively, and ψ is defocus parameter of the system. The optical transfer function (OTF) is the autocorrelation of the generalized pupil function, so one-dimensional OTF of the system can be expressed as

$$H(u,\psi) = \int P(k_1)\cdot\exp(\mathrm{i}\cdot k_1^2\cdot\psi)\cdot P(k_2)\cdot\exp(-\mathrm{i}\cdot k_2^2\cdot\psi)\,\mathrm{d}x,$$
$$k_1 = x+\frac{u}{2}, \quad k_2 = x-\frac{u}{2}, \tag{2}$$

where $H(u,\psi)$ is the OTF at one-dimensional spatial frequency u. Combining the theory of ambiguity function and stationary-phase method,[6] the relationship between the modulation transfer function (MTF) of optical system and defocus parameter is expressed by ambiguity function. Then we can derive the form of cubic phase mask (CPM) suitable for WFC system. To date, many phase masks, such as logarithmic phase mask,[13] tangent phase mask,[14] apodized CPM,[15] and others have been proposed. In this study, the conventional CPM is selected to realize our idea and the phase function of the conventional CPM can be expressed by

$$\varphi(x,y) = \alpha\cdot(x^3+y^3), \tag{3}$$

where α is the parameter of the CPM characterizing the phase modulation, has been proven to reduce the sensitivity of the PSF and MTF to defocus-related aberrations.[6,16] That is, WFC system shows good MTF consistency and PSF consistency. This is the theoretical basis of WFC technology. After encoding the image, the image can be restored using the digital de-convolution filter.

3. Establishing the optical structure of traditional infrared imager

3.1. Optical parameters of infrared imager

The F-number reflects the luminous flux capabilities of the optical system. The smaller the F-number, the more light energy enters the system per unit time, and the higher the brightness of the image surface.[17] A small F number can better meet the shooting requirements of infrared imagers in dark light environments. In this study, the F-number of the infrared imager is determined to be 1. At the same time, to meet the compact requirements of the infrared imager, the overall length of the optical structure is limited to 40 mm. Other optical parameters of the infrared imager are listed in Table 1.

Table 1. Parameters of the infrared optical system.

Term	Parameters value
Entrance pupil diameter	25 mm
F-number	1
Spectral range	8 μm–12 μm
Field of view	±16°
Pixel pitch	20 μm

Our starting point of lens design is a three-piece infrared optical system that is close to the parameter requirements, and the system is designed using the optical design software CODE V. The object is placed at infinity, and the materials of the lens are Ge, ZnSe, and Ge respectively. Taking the focal length and the overall length as specific constraints, the radius and thickness of each surface are set as variables, and then the standard optimization function and the global synthesis function of the software are activated successively. Among a series of reasonable structures obtained after optimization, we select the structure with the highest MTF of marginal FOV while ensuring on-axis MTF. The two-dimensional layout of the optical structure is given in Fig. 2.

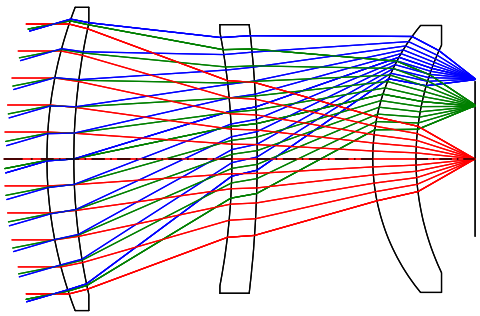


Fig. 2. Schematic diagram of the optical structure of infrared imager.

3.2. Aberration characteristics of traditional infrared imager

The MTF curve shows the change of the imaging modulation index of the optical system, which can reflect the transmission ability of the system to different frequency components of the object. The imaging quality of the optical system can be evaluated comprehensively through the MTF curve. The MTFs of the traditional infrared imager are shown in Fig. 3. Since only three spherical lenses are currently used, there are few optimization variables. At the marginal FOV, the MTFs can only reach 0.1 at 25 cycles/mm, which means that the optical system has serious aberrations.

Figure 4 illustrates the changes in the PSF of the traditional infrared imager at different FOV. To quantify the sensitivity of the optical system to aberrations, the Strehl ratio (SR)[18] is used as the index to evaluate image quality. As the FOV of system increases, the shapes and SR values of PSFs change severely, which means that traditional infrared imager is sensitive to changes in aberrations. This further indicates that the imaging quality of the traditional infrared imager is very poor, and it is difficult to achieve clear imaging by using only three spherical lenses. Traditional optical design methods typically require adding lens elements or introducing aspheric surfaces to improve image quality, which will increase the complexity of the optical system. In this study, a method of designing the infrared imager using WFC technology is proposed to improve the imaging quality while maintaining the simplicity of the optical system.

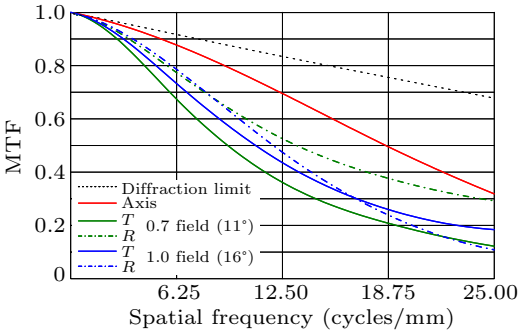


Fig. 3. MTFs of the traditional infrared imager at different FOV.

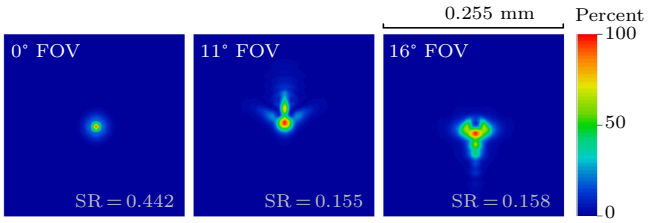


Fig. 4. PSFs of the traditional infrared imager at different FOV.

4. Design of infrared imager based on WFC technology

The WFC imaging system is insensitive to aberrations such as spherical aberration, coma and astigmatism.[8] Therefore, in this section, WFC technology is introduced into the design of the infrared imager to suppress aberrations.

4.1. The optimization of CPM parameters

While maintaining the optical structure of the traditional infrared imager in Fig. 2 unchanged, we attach the surface shape of the CPM to its pupil plane. Since the selection of the mask parameter will randomly degrade the performance of WFC imaging system, the mask parameter needs to be optimized to improve the imaging performance. We adopt a merit function based on the standard deviation (STD) of the PSF[8] to optimize the mask parameter. The merit function can be presented by

$$\mathrm{PARA} = \begin{cases} \mathrm{Minimize}\left\{ \dfrac{1}{X \cdot Y} \sum_{i}^{X} \sum_{j}^{Y} \dfrac{\mathrm{STD}[(\mathrm{PSF_{ZF}})_{i,j}]}{\mathrm{Mean}[(\mathrm{PSF_{ZF}})_{i,j}]} \right\}, \\ \mathrm{Subject\ to}\left\{ \int |H(\mathrm{u}, \mathrm{v}=0)|\, \mathrm{d}u \geq TH \right\}, \end{cases} \tag{4}$$

where PARA is the optimal parameter of the CPM, X and Y are sampling points for the entire PSF grid, $\mathrm{STD}\left[(\mathrm{PSF_{ZF}})_{i,j}\right]$ and

Mean$\left[(\mathrm{PSF}_{\mathrm{ZF}})_{i,j}\right]$ stand for the standard deviation and mean value of PSF at (i, j) of the full PSF grid at all sampled field positions, ZF stands for the position of different FOV, H stands for OTF of the WFC infrared imager and TH is the minimum acceptable average magnitude of MTF. According to the merit function shown in Eq. (4), the optimal mask parameter α for the CPM is 39.8, which is measured in radians.

4.2. Aberration characteristics and imaging performance of WFC infrared imager

Based on the optimal mask parameter, the PSFs for the WFC infrared imager at different FOV are given in Fig. 5. Despite the SR values are smaller than those in Fig. 4, the shapes of the PSFs in Fig. 5 are similar and the SR values are close at each FOV. It indicates that the WFC infrared imager is insensitive to the variation of aberrations. Therefore, the WFC technology has the potential to suppress aberrations of the infrared imager.

Image simulation is an intuitive way to evaluate the imaging performance of optical system. This section compares the simulated images of the traditional infrared imager and the WFC infrared imager at different FOV by using an infrared scene image. A Gaussian white noise model is used to simulate infrared noise.[19] Figure 6 is the original image of Gaussian white noise with a signal-to-noise ratio (SNR) of 10.

As shown in Fig. 7(a), the simulated images of the traditional infrared imager become blurry as the FOV increases. That means the high-frequency information is lost. Figure 7(b) shows the encoded images of the WFC infrared imager, which exhibits nearly uniform blurriness across the entire FOV, consistent with the characterization illustrated in Fig. 5. By using the digital de-convolution filter, the decoded images at different FOV are given in Fig. 7(c). The digital de-convolution filter is the Wiener filter and its expression is

$$F = \frac{H^*}{H^* \times H + K} = \frac{H^*}{|H|^2 + K}, \tag{5}$$

where K is a regularization parameter, H is the Fourier transform of the encoded PSF at 0° FOV and $*$ stands for complex conjugation operator.[8] The simulation result shows that the resolution and contrast of the images improve after applying Wiener filtering. In contrast to the traditional infrared imager, the WFC infrared imager maintains good imaging quality over a wide FOV.

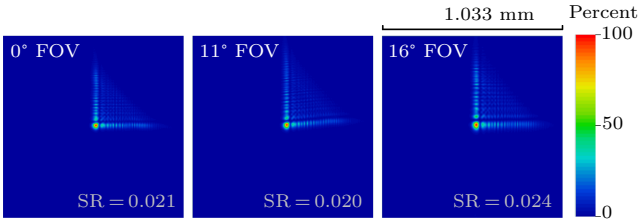


Fig. 5. PSFs of the WFC infrared imager at different FOV.

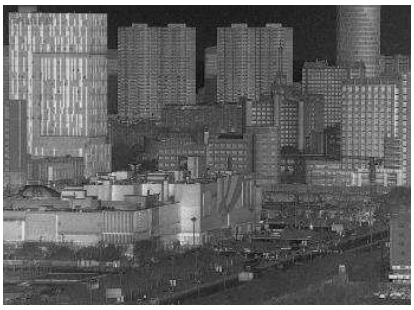


Fig. 6. Original image with an SNR = 10. Source of the original image: Raytron Technology Co., Ltd.

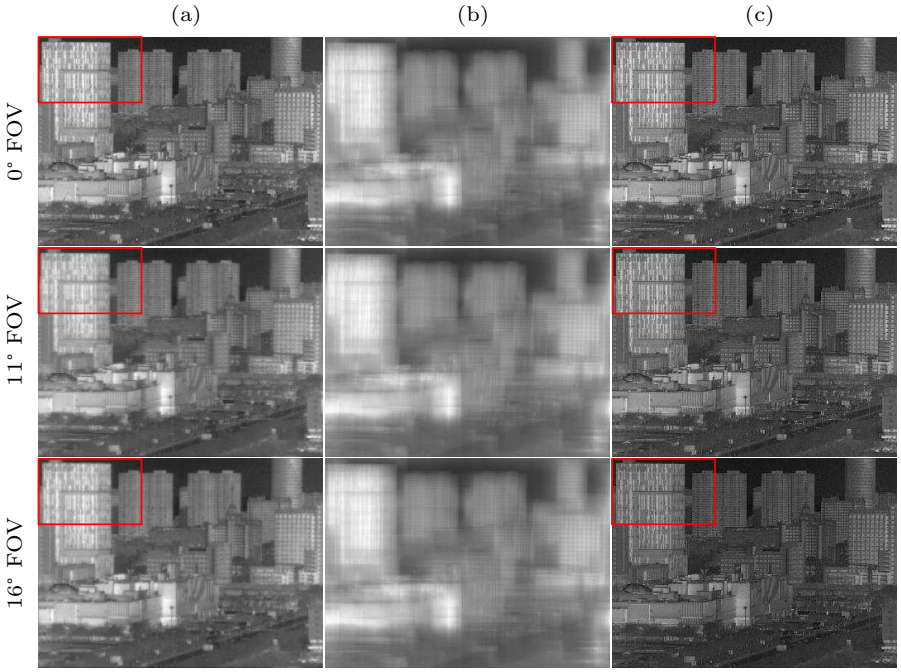


Fig. 7. Simulated results of infrared imagers. (a) Traditional infrared imager, (b) encoded images of WFC infrared imager, (c) decoded images of WFC infrared imager.

To quantify the quality of simulated images, we use the mean gradient (MG)[20] as the quantitative indicator of image clarity. The MG can sensitively reflect the ability of image to capture small details, and also reflect the characteristics of texture transformation in the image. In general, the larger the MG value, the more layers of the image, so the clearer the image. For a given image I, consisting of $M\times N$ pixels, its MG can be shown below:

$$\mathrm{MG}(I)=\frac{1}{M\times N}\sum_{i=1}^{M}\sum_{j=1}^{N}\sqrt{\frac{\left(\frac{\Delta I}{\Delta x}\right)_{ij}^{2}+\left(\frac{\Delta I}{\Delta y}\right)_{ij}^{2}}{2}}. \tag{6}$$

Based on the images in Fig. 7, the MG values of the simulated images of infrared imagers are shown in Table 2. It can be seen that the MG values of the decoded images are higher than those of the traditional infrared imager at each FOV. This result further demonstrates that the WFC infrared imager has better imaging quality in a wide FOV of $\pm16^\circ$.

The decoded MTFs of the WFC infrared imager are shown in Fig. 8. At 25 cycles/mm, the on-axis MTF is close to 0.6 and off-axis MTFs are both greater than 0.4, which indicates that the infrared imager has achieved high resolution by applying WFC technology.

Li *et al*. designed a three-piece long-wave infrared optical system using four aspheric surfaces, achieving a $\pm12^\circ$ FOV with an overall length under 32 mm.[21] The F-number of the infrared optical system is 1 and the focal length is 25 mm. At 25 cycles/mm, the on-axis MTF is greater than 0.6 and off-axis MTFs are both greater than 0.3. Compared with Ref. [21], although the overall length of our design is slightly longer, it achieves a wider FOV and higher off-axis MTFs. In addition, the surface shapes of the WFC infrared imager are spherical lenses except for the pupil plane. As a result, the structure of the infrared optical system is simplified, which could relax the alignment and fabrication tolerances and improve the stability of the system to a certain extent. This is of great significance for infrared imagers applied in military surveillance or night navigation.

Table 2. MG values of the simulated images of infrared imagers at different FOV.

MG	0° FOV	11° FOV	16° FOV
Images of traditional infrared imager	2.236	1.605	1.504
WFC encoded images	0.808	0.743	0.748
WFC decoded images	4.065	3.855	3.626

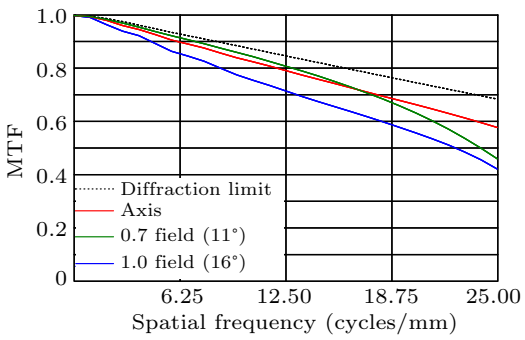


Fig. 8. Decoded MTFs of WFC infrared imager at different FOV.

5. Summary and conclusion

In this paper, we design a three-piece compact wide-FOV infrared imager using WFC technology. The optical structure of a traditional infrared imager is established and its aberration characteristics are analyzed. The traditional infrared imager uses only three spherical lenses, which limits the design degrees of freedom, resulting in poor imaging quality. While maintaining the optical structure of the traditional infrared imager unchanged, the CPM is inserted in its pupil plane to suppress aberrations. By using evaluation methods such as PSF, MTF and image simulation, the WFC infrared imager with a CPM has better imaging performance than the traditional infrared imager. Compared with another traditional design method using four aspheric surfaces, the infrared imager using WFC technology not only achieves a wider FOV and higher off-axis MTFs, but also simplifies the structure of the infrared optical system, thus relaxing the alignment and fabrication tolerances and improving the stability of the system. This study provides a new strategy for the design of compact infrared imagers with a wide FOV. The complete design and detailed simulation verification proposed in this paper provide a reliable basis for subsequent experimental verification, which is our next research direction.

References

[1] Ye J F, Yu J, Song Z Z, Pei S X, Yuan Q, Gao Z S and He Y 2019 *J. Mod. Opt.* **66** 304

[2] Li Q Y, Zhang Y, Yan S Y, Zhang B and Wang C H 2022 *Chin. Phys. B* **31** 074201

[3] Wu Q, Zhang S S, Liao W X, Xu W B, Wang T S, Zhang H X and Shi C Y 2022 *Opt. Express* **30** 45143

[4] Shearer A, Hauke B, Montazerian M and Mauro J C 2023 *Optical Materials: X* **20** 100258

[5] Khatri N, Berwal S, Singh B, Tewary S, Manjunath K and Goel S 2025 *J. Manuf. Processes* **142** 468

[6] Dowski E R and Cathey W T 1995 *Appl. Opt.* **34** 1859

[7] Colburn S, Zhan A and Majumdar A 2018 *Sci. Adv.* **4** eaar2114

[8] Yu J Q, Chen S Q, Dang F Y, Li X S, Shi X T, Ju L, Wang H, Xu X M and Fan Z G 2020 *Opt. Commun.* **463** 125121

[9] Ma L F, Du S, Chang J, Chen W L, Wu C H, Shi X X, Huang Y, Zhong Y and Mu Q Q 2023 *Chin. Phys. B* **32** 084201

[10] Feng B, Shi Z L, Chang Z, Liu H Z and Zhao Y H 2017 *Infrared Phys. Technol.* **85** 157

[11] Zhou J, Chen S Q, Zhen Z, Ou W and Xiong J 2020 *Infrared and Laser Engineering* **49** 0404001 (in Chinese)

[12] Wang W, Zhang L H and Fu T W 2023 *Laser Optoelectron. Prog.* **60** 1011005 (in Chinese)

[13] Zhao H and Li Y C 2010 *Opt. Lett.* **35** 2630

[14] Le V N, Chen S Q and Fan Z G 2014 *Opt. Lett.* **39** 2171

[15] Zhu L N, Li F, Huang Z Y and Zhao T Y 2022 *Chin. Phys. B* **31** 054217

[16] Bradburn S, Cathey W T and Dowski E R 1997 *Appl. Opt.* **36** 9157

[17] Smith W 2000 *Modern Optical Engineering: The Design of Optical Systems* (New York: McGraw-Hill Companies) pp. 151-153

[18] Yu J Q, Chen S Q, Dang F Y, Li X S, Shi X T, Wang H and Fan Z G 2021 *Opt. Commun.* **490** 126876

[19] Wang Y, Xie X F, Zhang L and Yang J 2015 *Laser & Infrared* 45 1277

[20] Qiao C, Li D, Guo Y, Liu C, Jiang T, Dai Q and Li D 2021 *Nat. Methods* **18** 194

[21] Yang J Q, Peng Q Q, Liu L, Li R G and Sun C F 2017 *Laser & Infrared* **47** 225